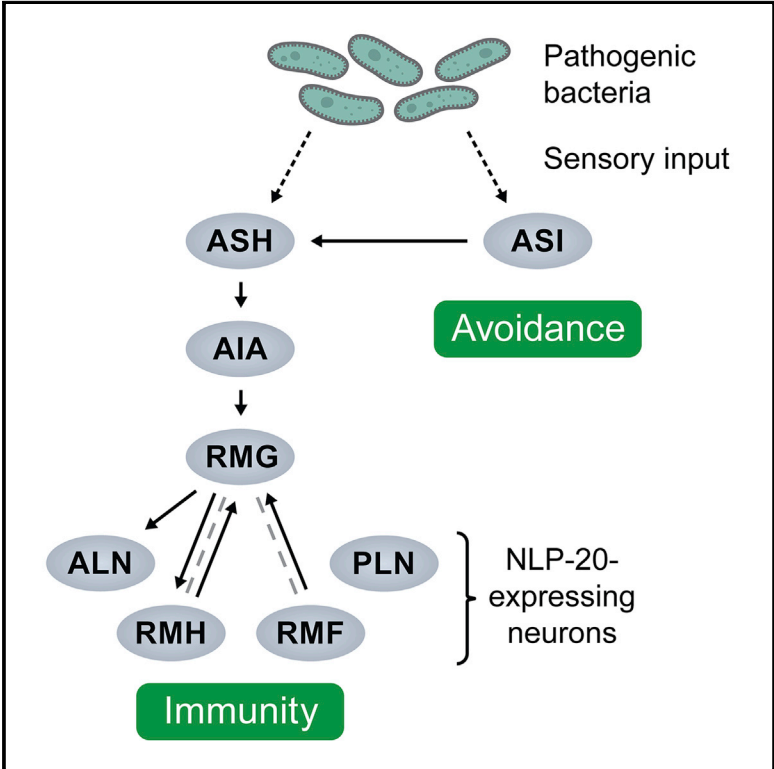


Distinct Roles of Sensory Neurons in Mediating Pathogen Avoidance and Neuropeptide-Dependent Immune Regulation

Graphical Abstract



Authors

Xiou Cao, Rie Kajino-Sakamoto, Argenia Doss, Alejandro Aballay

Correspondence

aballay@ohsu.edu

In Brief

Cao et al. show that chemosensory neurons have the ability to coordinate behavioral and immune responses upon bacterial infections in *C. elegans*. The underlying mechanisms involve interneurons and neuropeptide signaling and provide insights into tactics that may be used by animals when dealing with pathogen threats.

Highlights

- ASI sensory neurons promote pathogen avoidance to pathogenic bacteria
- ASH sensory neurons control the innate immune pathways in *C. elegans*
- Neuropeptide NLP-20 functions downstream of OCTR-1 in controlling immunity
- AIA neurons link ASH neurons and NLP-20-expressing neurons in the control of immunity



Distinct Roles of Sensory Neurons in Mediating Pathogen Avoidance and Neuropeptide-Dependent Immune Regulation

Xiou Cao,¹ Rie Kajino-Sakamoto,^{1,2} Argenia Doss,¹ and Alejandro Aballay^{1,3,4,*}

¹Department of Molecular Genetics and Microbiology, Duke University Medical Center, Durham, NC 27710, USA

²Division of Molecular Pathology, Aichi Cancer Center Research Institute, Nagoya, Aichi 464-8681, Japan

³Department of Molecular Microbiology & Immunology, Oregon Health & Science University, Portland, OR 97239, USA

⁴Lead Contact

*Correspondence: aballay@ohsu.edu

<https://doi.org/10.1016/j.celrep.2017.10.050>

SUMMARY

Increasing evidence implies an extensive and universal interaction between the immune system and the nervous system. Previous studies showed that OCTR-1, a neuronal G-protein-coupled receptor (GPCR) analogous to human norepinephrine receptors, functions in sensory neurons to control the gene expression of both microbial killing pathways and the unfolded protein response (UPR) in *Caenorhabditis elegans*. Here, we found that OCTR-1-expressing neurons, ASH, are involved in controlling innate immune pathways. In contrast, another group of OCTR-1-expressing neurons, ASI, was shown to promote pathogen avoidance behavior. We also identified neuropeptide NLP-20 and AIA interneurons, which are responsible for the integration of conflicting cues and behaviors, as downstream components of the ASH/ASI neural circuit. These findings provide insights into a neuronal network involved in regulating pathogen defense mechanisms in *C. elegans* and might have broad implications for the strategies utilized by metazoans to balance the energy-costly immune activation and behavioral response.

INTRODUCTION

The competition between host and pathogen is considered to be an important driving force of evolution, promoting the emergence of the immune system, which comprises a variety of specialized cells and organs (Flajnik and Kasahara, 2010; Sironi et al., 2015). Upon pathogen infection, the immune system initiates the corresponding immune response and provides the host with significant advantages by employing a series of sophisticated molecular and cellular mechanisms to eliminate infectious agents and restore normal physiological activities (Akira et al., 2006; Iwasaki and Medzhitov, 2010; Pancer and Cooper, 2006). Nonetheless, activation of the immune response in-

creases demands on protein synthesis and energy consumption, which are mitigated by the induction of stress response pathways such as the unfolded protein response (UPR) to achieve immune homeostasis (Grootjans et al., 2016). In addition, many animal species, including humans, have developed the so-called “behavioral immune response” to detect aversive sensory cues and avoid potential threats by reducing contact with pathogens (Curtis, 2014; Kavaliers and Choleris, 2011; Meisel and Kim, 2014). The proper coordination of these defense mechanisms appears to be a pivotal task of animals to manage pathogenic assaults in their natural habitat.

Recent studies using the model organism *Caenorhabditis elegans* have highlighted the role of neural G-protein-coupled receptors (GPCRs) in controlling immune mechanisms and pathogen avoidance behavior against pathogen infections (Cao and Aballay, 2016; Reddy et al., 2009; Styer et al., 2008; Sun et al., 2011). GPCRs are an important group of molecules that function in the nervous system to transduce signals and modulate neuronal responses to environmental stimuli (Lefkowitz, 2013). In *C. elegans*, GPCR NPR-1, a homolog of human neuropeptide Y receptor, has been shown to control both immunity and oxygen-dependent avoidance behavior, which participates in pathogen infection (Martin et al., 2017; Reddy et al., 2009; Styer et al., 2008). Thus, the perception of pathogens by the sensory system appears to be followed by immune and behavioral responses that balance the requirements for food uptake, energy storage, and pathogen containment. In addition, an octopamine receptor, OCTR-1, has been found to regulate the immune response of *C. elegans* by inhibiting the expression of effector genes of the conserved PMK-1/p38 mitogen-activated protein kinase (MAPK) pathway and the X-box binding protein 1 (XBP-1) branch of the canonical UPR pathway (Sun et al., 2012, 2011). Further studies have revealed that OCTR-1 functions in ASH and ASI sensory neurons to control the expression of immune-related genes and contribute to survival of infection by pathogenic bacteria (Sun et al., 2011).

Here we show that the sensory neurons ASH and ASI have distinct roles in mediating pathogen defense mechanisms. Upon pathogen infection, ASI neurons function to promote pathogen avoidance, whereas ASH neurons downregulate immunity by inhibiting the expression of immune-related factors. We also show that a neuropeptide gene, *nlp-20*, which is expressed in

several head and tail neurons, is required for enhanced resistance to pathogen infection and upregulation of immune and UPR genes in *octr-1(ok371)* animals. We further demonstrate that AIA interneurons might act as key players linking ASH neurons and NLP-20-expressing neurons to mediate immune regulation. These findings suggest a neuronal network by which *C. elegans* controls immune activation and proteostasis and provide evidence for the neural strategies of the animals to effectively coordinate behavioral and immune responses against pathogen infection.

RESULTS

ASI Neurons Promote Avoidance to the Pathogen

P. aeruginosa

The amphid sensory neurons of *C. elegans* have been known to regulate a series of physiological processes such as chemotaxis, aversive learning, and longevity (Inglis et al., 2007). To determine the specific role of amphid sensory neurons in controlling microbial defense mechanisms, we decided to perform single-neuron ablation of each amphid sensory neuron expressing OCTR-1. First, we took advantage of strain PY7505, which was generated by expressing the two subunits of the *C. elegans* caspase CED-3 (p15 and p17) under the promoters of the genes *gpa-4* and *gcy-27* to induce programmed cell death in ASI neurons (Beverly et al., 2011; Gallagher et al., 2013). To determine whether ASI neurons play a role in controlling innate immunity, we subjected ASI(–) animals to infection by the bacterial pathogen *P. aeruginosa*. We found that ASI(–) animals exhibited enhanced susceptibility to *P. aeruginosa* infection compared with wild-type animals, whereas their lifespan is slightly but significantly longer than that of wild-type animals when grown on non-pathogenic *E. coli* (Figure 1A; Figure S1A). This suggests that ablation of ASI sensory neurons does not shorten the life of *C. elegans* but, rather, affects its defense mechanism against pathogenic bacteria. In addition, the enhanced resistance to infection of *octr-1(ok371)* animals was suppressed by ablation of ASI neurons (Figure 1A). *C. elegans* naturally exhibits an avoidance behavior when exposed to *P. aeruginosa*, which can be observed under conditions where the animals can freely enter and exit the bacterial lawn. When we used plates that were completely covered by bacteria to control for avoidance (full lawn), the survival of ASI(–) animals was comparable with that of wild-type animals (Figure 1B). Because the assay using full lawns eliminates the contribution of avoidance behavior to resist pathogen infection, the lack of susceptibility of ASI(–) animals indicates that ASI sensory neurons promote avoidance behavior upon pathogen infection. Consistent with this notion, we also found that there was no significant difference between the resistance of *octr-1(ok371)* and ASI(–);*octr-1(ok371)* animals on plates covered by full-lawn pathogenic bacteria (Figure 1B). Therefore, we directly assessed whether ASI neurons were involved in the avoidance response to *P. aeruginosa* by performing a lawn occupancy assay in which we calculated the fraction of animals on the bacterial lawn after being placed on *P. aeruginosa* for 24 hr. Both ASI(–) and ASI(–);*octr-1(ok371)* animals showed a higher percentage of lawn occupancy compared with wild-type animals,

indicating that ASI neurons indeed promote pathogen avoidance in *C. elegans* (Figure 1C).

ASH Neurons Inhibit Innate Immunity in *C. elegans*

Because the expression of OCTR-1 in ASI and ASH neurons confers immune suppression, and ASI neurons regulate pathogen avoidance behavior, we next questioned whether ASH neurons are involved in immune modulation in *C. elegans*. We used a strain of *C. elegans* in which ASH neurons were ablated by expressing the caspase CED-3 under the promoter of the gene *sra-6* (Choi et al., 2015). We found that ASH(–) animals showed enhanced resistance to pathogen infection on both partial and full lawns of *P. aeruginosa* (Figures 1D and 1E). In addition, ASH(–) animals did not show a different lifespan or pathogen avoidance behavior compared with wild-type animals (Figure 1F; Figure S1B). These data suggest that, in contrast to ASI neurons, ASH neurons downregulate the immune response without affecting pathogen avoidance behavior in *C. elegans*. To further validate this idea, we also performed qRT-PCR to assess the expression level of the PMK-1-dependent genes (Troemel et al., 2006) and the UPR genes (Urano et al., 2002), which are known to be upregulated in *octr-1(ok371)* animals. Marker genes of both the PMK-1 pathway and the XBP-1 canonical UPR pathway were upregulated in ASH(–) animals but not in ASI(–) animals (Figures 1G and 1H; Figures S1C and S1D). In addition, there were no significant differences in survival between *octr-1(ok371)* and ASH(–);*octr-1(ok371)* animals, suggesting that ASH but not ASI neurons are responsible for controlling immune-related gene expression (Figures 1D and 1E).

Neuropeptide NLP-20 Is Required for OCTR-1-Mediated Immune Regulation

By performing whole-genome expression analysis, we have shown that OCTR-1 downregulates important immune pathways in *C. elegans*, such as the PMK-1/p38 and DAF-16/insulin pathways (Sun et al., 2011). The same study further indicates that a neuropeptide-like protein (*nlp*) gene, *nlp-20*, is also upregulated in *octr-1(ok371)* animals, suggesting that neuropeptides may play a role in mediating immune regulation in *C. elegans* (Figure S2A). To test this hypothesis, we first used qRT-PCR to verify the whole-genome expression analysis and found that the *nlp-20* gene was indeed upregulated in *octr-1(ok371)* animals as well as in ASH(–) and ASH(–);*octr-1(ok371)* animals (Figure 2A). To examine whether *nlp-20* controls the innate immune response of *C. elegans*, we exposed *nlp-20(ok1591)* mutant animals to partial pathogen lawns of *P. aeruginosa*. We found that *nlp-20(ok1591)* animals showed a survival rate comparable with wild-type animals on pathogen lawns (Figure 2B). However, the *nlp-20* mutation completely suppressed the enhanced resistance to *P. aeruginosa*-mediated killing of *octr-1(ok371)* animals, indicating that *nlp-20* is required for the enhanced immune response of *octr-1(ok371)* mutants (Figure 2B). As mentioned above, nematodes exhibit a behavioral response to live *P. aeruginosa* and avoid lawns of *P. aeruginosa* when they are infected. To explore whether the lack of pathogen avoidance might contribute to the reduced resistance of *octr-1(ok371);nlp-20(ok1591)* double mutants, we challenged the animals by using

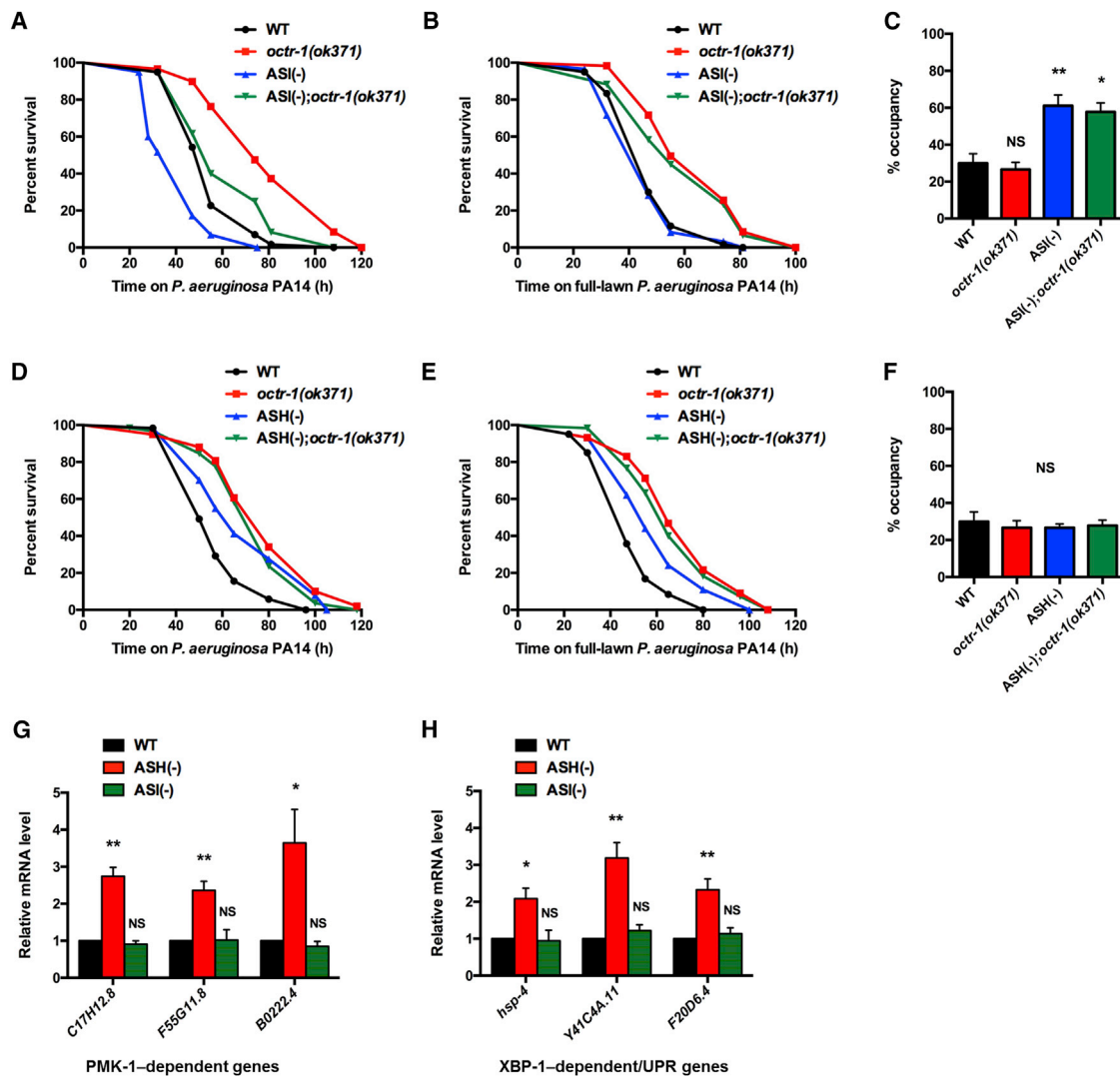


Figure 1. The Distinct Roles of OCTR-1-Expressing Neurons in Combating Bacterial Invasion

(A) Wild-type, *octr-1(ok371)*, ASI(-), and ASI(-);*octr-1(ok371)* animals were exposed to partial lawns of *P. aeruginosa* PA14 and scored for survival. Wild-type (WT) versus ASI(-), $p < 0.001$; ASI(-) versus ASI(-);*octr-1*, $p < 0.001$.

(B) WT, *octr-1(ok371)*, ASI(-), and ASI(-);*octr-1(ok371)* animals were exposed to full lawns of *P. aeruginosa* PA14 and scored for survival. WT versus ASI(-), $p > 0.1$; ASI(-) versus ASI(-);*octr-1*, $p > 0.1$.

(C) WT, *octr-1(ok371)*, ASI(-), and ASI(-);*octr-1(ok371)* animals were cultured on partial pathogen lawns, and the percentages of animals on the pathogen lawns after incubation for 24 hr were calculated.

(D) WT, *octr-1(ok371)*, ASH(-), and ASH(-);*octr-1(ok371)* animals were exposed to partial lawns of *P. aeruginosa* PA14 and scored for survival. WT versus ASH(-), $p < 0.01$; *octr-1* versus ASH(-);*octr-1*, $p > 0.1$.

(E) WT, *octr-1(ok371)*, ASH(-), and ASH(-);*octr-1(ok371)* animals were exposed to full lawns of *P. aeruginosa* PA14 and scored for survival. WT versus ASH(-), $p < 0.05$; *octr-1* versus ASH(-);*octr-1*, $p > 0.1$.

(F) WT, *octr-1(ok371)*, ASH(-), and ASH(-);*octr-1(ok371)* animals were cultured on partial pathogen lawns, and the percentages of animals on the pathogen lawns after incubation for 24 hr were calculated.

(G) qRT-PCR analysis of PMK-1-dependent genes in ASI(-) and ASH(-) compared with WT animals.

(H) qRT-PCR analysis of XBP-1-dependent genes in ASI(-) and ASH(-) compared with WT animals.

See also Figure S1.

full-lawn bacterial plates, which eliminated the possibility of pathogen avoidance. Similarly, no difference in the survival rate of *nlp-20(ok1591)* and wild-type animals was observed on full-lawn plates, and the *nlp-20* mutation was still able to abolish the enhanced resistance to pathogen infection of *octr-1(ok371)*

animals (Figure 2C). Furthermore, we monitored the lawn occupancy of the animals and observed no defects related to pathogen avoidance behavior, indicating that *nlp-20* does not play a role in controlling pathogen avoidance behavior (Figure 2D). In addition, expression of *nlp-20* under its own promoter rescued

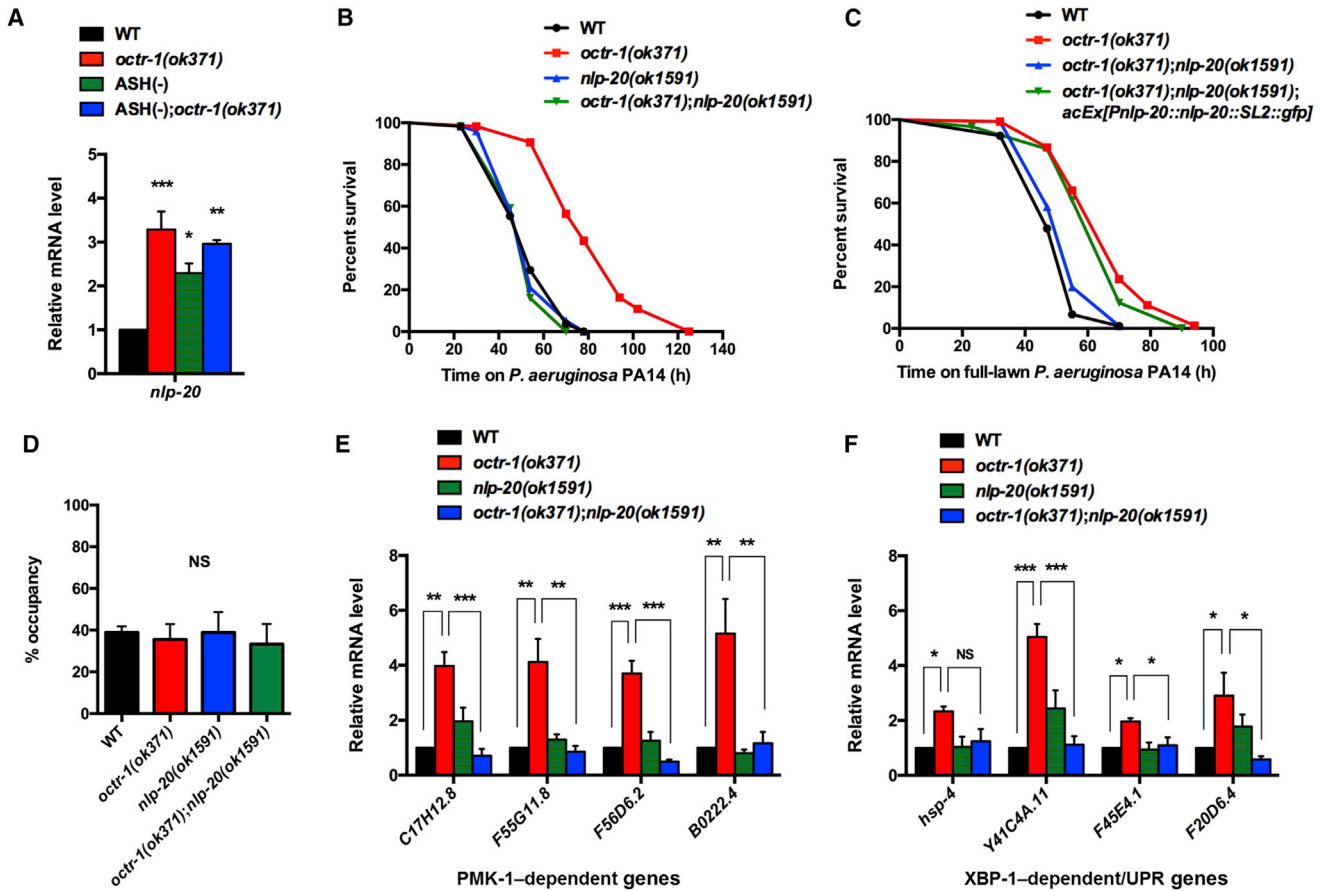


Figure 2. The Neuropeptide NLP-20 Is Involved in the Immune Regulation Mediated by OCTR-1

(A) qRT-PCR analysis of the expression of *nlp-20* in *octr-1(ok371)*, ASH(-), and ASH(-);*octr-1(ok371)* animals compared with WT animals. (B) WT, *octr-1(ok371)*, *nlp-20(ok1591)*, and *octr-1(ok371);nlp-20(ok1591)* animals were exposed to partial lawns of *P. aeruginosa* PA14 and scored for survival. *nlp-20* versus *octr-1;nlp-20*, $p < 0.0001$. (C) WT, *octr-1(ok371)*, *octr-1(ok371);nlp-20(ok1591)*, and *octr-1(ok371);nlp-20(ok1591);acEx[Pnlp-20::nlp-20::SL2::gfp]* animals were exposed to full lawns of *P. aeruginosa* PA14 and scored for survival. *nlp-20* versus *octr-1;nlp-20*, $p < 0.001$; *octr-1;nlp-20* versus *octr-1;nlp-20;acEx[Pnlp-20::nlp-20::SL2::gfp]*, $p < 0.01$. (D) WT, *octr-1(ok371)*, *nlp-20(ok1591)*, and *octr-1(ok371);nlp-20(ok1591)* animals were cultured on partial pathogen lawns, and the percentages of animals on the pathogen lawns after incubation for 24 hr were calculated. (E) qRT-PCR analysis of PMK-1-dependent genes in *octr-1(ok371)*, *nlp-20(ok1591)*, and *octr-1(ok371);nlp-20(ok1591)* animals compared with WT animals. (F) qRT-PCR analysis of XBP-1-dependent genes in *octr-1(ok371)*, *nlp-20(ok1591)*, and *octr-1(ok371);nlp-20(ok1591)* animals compared with WT animals. See also Figure S2.

the deficient survival of the *octr-1(ok371);nlp-20(ok1591)* double mutant to levels that were comparable with those of *octr-1(ok371)* animals (Figure 2C). Taken together, these data suggest that *nlp-20* functions downstream of *octr-1* and is required for the enhanced survival of *octr-1(ok371)* animals without affecting behavioral responses to the pathogen.

It has been shown that OCTR-1 inhibits activation of the PMK-1/p38 MAPK pathway and, thus, downregulates the expression of PMK-1-dependent genes (Sun et al., 2011). To assess whether the mutation in the *nlp-20* gene also suppresses the effect of OCTR-1 on the expression of PMK-1-dependent genes, we performed qRT-PCR assays to analyze the expression of several marker genes of the PMK-1/p38 MAPK pathway that have been shown to be induced in *octr-1(ok371)* animals

(Sun et al., 2011). As shown in Figure 2E and Figure S2B, the upregulation of PMK-1-dependent genes in the *octr-1(ok371)* mutant was significantly suppressed by *nlp-20* mutation to levels comparable with that in wild-type animals, suggesting that *nlp-20* is required for the increased level of PMK-1-dependent genes in *octr-1(ok371)* animals. It is known that OCTR-1 acquires the control of the XBP-1 branch of the canonical UPR during development and that marker genes of this pathway, such as *hsp-4*, are upregulated in *octr-1(ok371)* animals at a young adult stage (Sun et al., 2012). Similar to the suppression of PMK-1-dependent genes, the expression levels of XBP-1-dependent genes in young adults were significantly reduced to basal levels in the *octr-1(ok371);nlp-20(ok1591)* double mutant, suggesting that *nlp-20* is also involved in controlling the XBP-1 branch of the

canonical UPR pathway and contributes to the OCTR-1-mediated immune regulation (Figure 2F; Figure S2C).

Neuropeptide NLP-20 Is Expressed in Several Head and Tail Neurons

To determine the expression pattern of the *nlp-20* gene, we expressed GFP driven by the 2-kb promoter of the *nlp-20* gene in wild-type animals. The transgene *Pnlp-20::gfp* was strongly expressed in four head neurons that were likely to be two of the four paired neurons AIA, RMF, RMH, and RMDD (Figures 3A and 3B). The NLP-20-expressing cells did not overlap with the cells expressing the gene *mgl-1*, which has been shown to be expressed in AIA, RMDV, RMDD, and NSM neurons (Figures S3A–S3C; Greer et al., 2008). These results indicated that RMF and RMH might be the cells expressing GFP under the control of the *nlp-20* promoter. We further confirmed this result by co-expressing *Pnlp-20::gfp* with mCherry driven by the promoter of the *ser-1* gene, which is known to be expressed in several types of cells, including five pairs of head neurons (CEP, RMG, RMH, RMF, and RMD) (Xiao et al., 2006). The cells expressing *Pnlp-20::gfp* co-localized with the reporter *Pser-1::mCherry* only in RMF or RMH neurons (Figures S3D–S3F). In addition, the other four cells with cell bodies located in the tail also expressed *nlp-20* (Figures 3C and 3D). The two anterior cells were near the two PHA and PHB phasmid neurons (Figures 3E and 3F). The anterior nerve process projecting out of two tail neurons seemed to join the ventral sublateral cords at approximately mid-body (Figures 3G and 3H), which is a distinctive feature of the PLN left and right neurons; the other pair of tail neurons may represent ALN neurons. In addition to these NLP-20-expressing cells, occasional expression in four cells in the head was also noted (data not shown). To evaluate the immune function of NLP-20-expressing neurons, we expressed CED-3 caspase under the promoter *nlp-20* to induce neurodegeneration and found that ablation of these neurons could partially suppress the enhanced resistance to pathogen infection of *octr-1(ok371)* animals, indicating that these neurons are involved in immune regulation mediated by OCTR-1 (Figure 3I).

AIA Interneurons Function Downstream of OCTR-1 and Link ASH Neurons to NLP-20-Expressing Neurons

There are no described synaptic connections between ASH neurons and NLP-20-expressing neurons (White et al., 1986). To dissect the neural circuit involved in the mechanism by which ASH neurons control the expression level of *nlp-20* upon pathogen infection, we took advantage of the existing neuronal diagram in *C. elegans* and constructed a neural network incorporating both ASH neurons and NLP-20-expressing neurons (Figure 3J). In the diagram, we found that AIA interneurons lie between these two subsets of neurons and might act as a functional link. In addition, AIA interneurons have been shown to be responsible for the integration of conflicting sensory cues and behavior choice (Shinkai et al., 2011; Tomioka et al., 2006). We speculated that AIA neurons may function as a group of interneurons for transmitting immune-regulatory signals originating from ASH neurons to downstream NLP-20-expressing neurons.

To test this hypothesis, we used an AIA-ablated strain in which a hyperactive form of a DEG/ENaC sodium channel, MEC-4, is

expressed under the promoter of the gene isoform *gcy-28.d* to induce degeneration in AIA neurons (Shinkai et al., 2011). We investigated the expression level of *nlp-20* upon ablation of AIA neurons and discovered that the expression of *nlp-20* in AIA(–) animals was comparable with that of wild-type animals (Figure 4A). Importantly, although induced in *octr-1(ok371)* animals, the expression of *nlp-20* was significantly suppressed in AIA(–);*octr-1(ok371)* animals, suggesting that AIA interneurons are essential for the upregulation of *nlp-20* induced in the absence of *octr-1* (Figure 4A).

To further investigate the role of AIA neurons in mediating pathogen defense, we performed survival assays in which animals were subjected to either partial or full lawns of the pathogen *P. aeruginosa*. We found that AIA(–) animals showed susceptibility comparable with wild-type animals under both conditions of infection and did not show any longevity phenotype (Figures 4B and 4C; Figure S4A). More importantly, the ablation of AIA neurons completely suppressed the enhanced resistance to pathogen infection of *octr-1(ok371)* animals (Figures 4B and 4C). In addition, no significant pathogen avoidance was observed for AIA(–) and AIA(–);*octr-1(ok371)* compared with wild-type animals (Figure 4D). These data suggest that AIA neurons promote the survival of *octr-1(ok371)* animals by regulating immunity but not behavioral responses upon pathogen infection. Consistent with this notion, we found that the ablation of AIA neurons significantly suppressed the upregulation of marker genes of the PMK-1/p38 MAPK pathway as well as the XBP-1 branch of the UPR, the two groups of immune-related genes controlled by OCTR-1 (Figures 4E and 4F; Figures S4B and S4C). Taken together, these results indicate that AIA interneurons are key players in mediating the OCTR-1-controlled immune response and might serve to link the immune-regulatory neural circuit containing ASH and NLP-20-expressing neurons.

DISCUSSION

Our findings established the molecular and neuronal basis by which two different sets of neurons, ASI and ASH, coordinate responses against pathogen infection either by using microbial killing mechanisms or pathogen avoidance. Specifically, we showed that the OCTR-1-expressing neurons ASI and ASH have distinct functions in mediating the defense response to *P. aeruginosa*: ASI neurons activate pathogen avoidance behavior, and ASH neurons negatively control the PMK-1/p38 MAPK pathway and the XBP-1 branch of the UPR pathway. ASI neurons are known to control dauer formation and chemotaxis, whereas ASH neurons regulate nociception, such as osmotic avoidance, chemical avoidance, and social feeding. Recent studies indicate the presence of a reciprocal inhibitory neural circuit comprising the ASI and ASH neurons in *C. elegans* to modulate Cu^{2+} nociception and avoidance behavior (Guo et al., 2015). In addition, there are synaptic connections between ASH and ASI neurons, suggesting that these two neurons might work collaboratively to coordinate behavior, development, energy consumption, and immunity in response to danger signals from the environment, such as pathogenic bacteria (Figure 4G). Other amphid sensory neurons have also been shown to control pathogen avoidance behavior: AWB

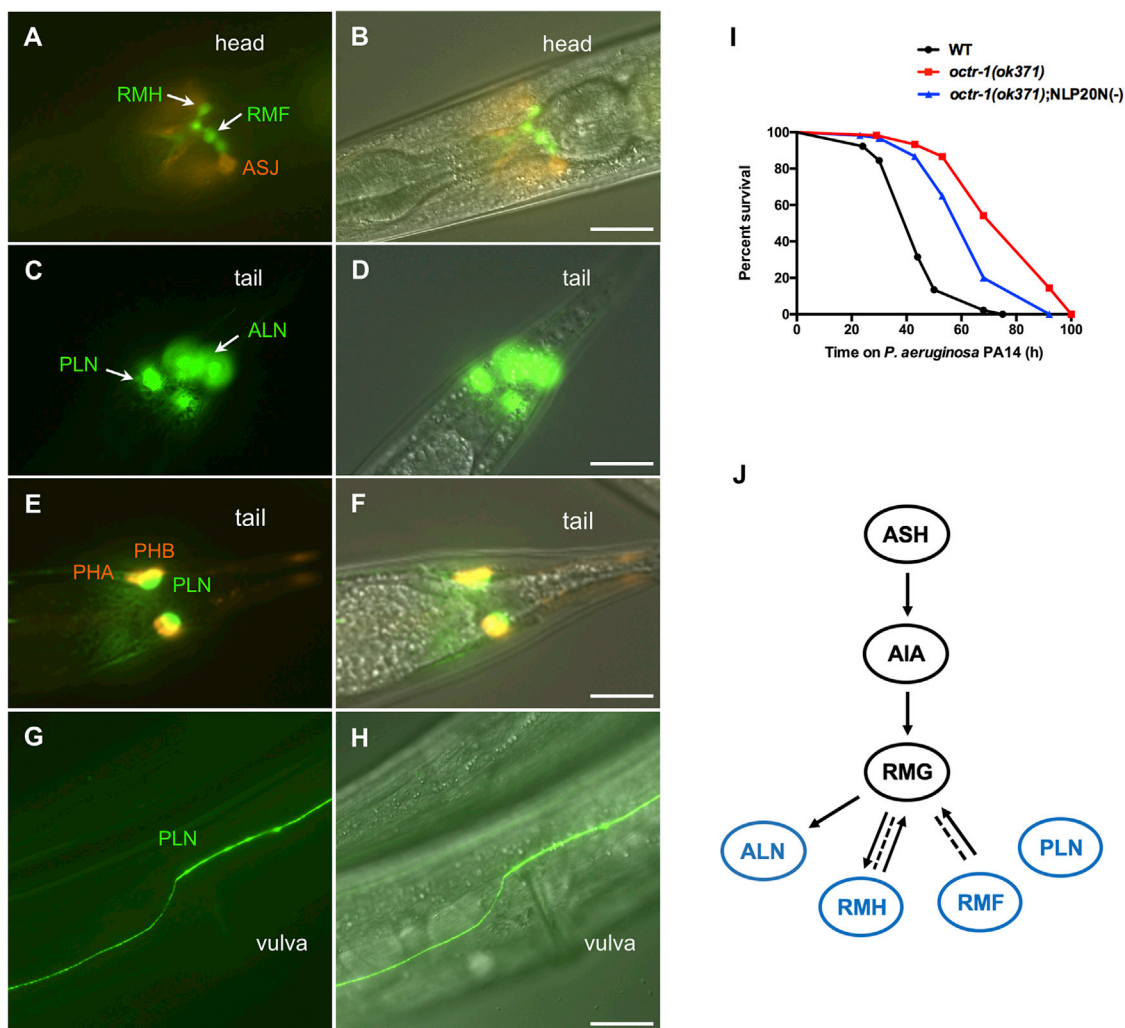


Figure 3. Neurons Expressing *nlp-20* Are Required for the Enhanced Immunity of *octr-1(ok371)* Animals

(A–H) Young adult WT animals carrying the *Pnlp-20::gfp* transgene were visualized using a fluorescence microscope to identify neurons expressing *nlp-20*. Fluorescence images were merged with their corresponding differential interference contrast (DIC) images. Scale bar, 20 μ m.

(A and B) Expression of *Pnlp-20::gfp* was detected in four head neurons. The two neurons in the middle are RMH neurons; the other two neurons lying outside are RMF neurons. The ASJ amphid neuron was visualized by DiD. Other labeled amphid neurons were not visible in this focal plane. (A) Fluorescence image and (B) DIC image.

(C and D) *Pnlp-20::gfp* was expressed in four neurons with cell bodies located in the tail (ALN and PLN neurons). The images were unfocused to show all four cell bodies. (C) Fluorescence image and (D) DIC image.

(E and F) The anterior two cells (PLN neurons) expressing *nlp-20* were located near PHA and PHB phasmid neurons, which were labeled with DiD. (E) Fluorescence image and (F) DIC image.

(G and H) Anterior axon migration of PLN neurons around the vulva showing the commissure that directs the process of the neuron to the ventral sublateral cords. Left, anterior; right, posterior. (G) Fluorescence image and (H) DIC image.

(I) WT, *octr-1(ok371)*, and *octr-1(ok371);NLP-20N(-)* animals were exposed to partial lawns of *P. aeruginosa* PA14 and scored for survival. *octr-1* versus *octr-1;NLP-20N(-)*, $p < 0.05$.

(J) Neuronal wiring diagram showing synaptic connectivity. AIA interneurons serve as a linker between ASH neurons and NLP-20-expressing neurons (labeled in blue), including ALN, RMH, and RMF neurons.

See also Figure S3.

neurons are responsible for the avoidance of *S. marcescens* (Pradel et al., 2007), and ASJ neurons are able to detect the secondary metabolites of *P. aeruginosa*, which induce the cell-autonomous expression of DAF-7 to control pathogen avoidance behavior through a canonical transforming growth

factor β (TGF- β) signaling (Meisel et al., 2014). The lack-of-avoidance phenotype of *daf-7* mutant could be fully rescued by expressing *daf-7* in either ASJ neurons or ASI neurons. Furthermore, animals with ablated ASJ neurons do not show avoidance comparable with *daf-7* mutants, suggesting a putative role for

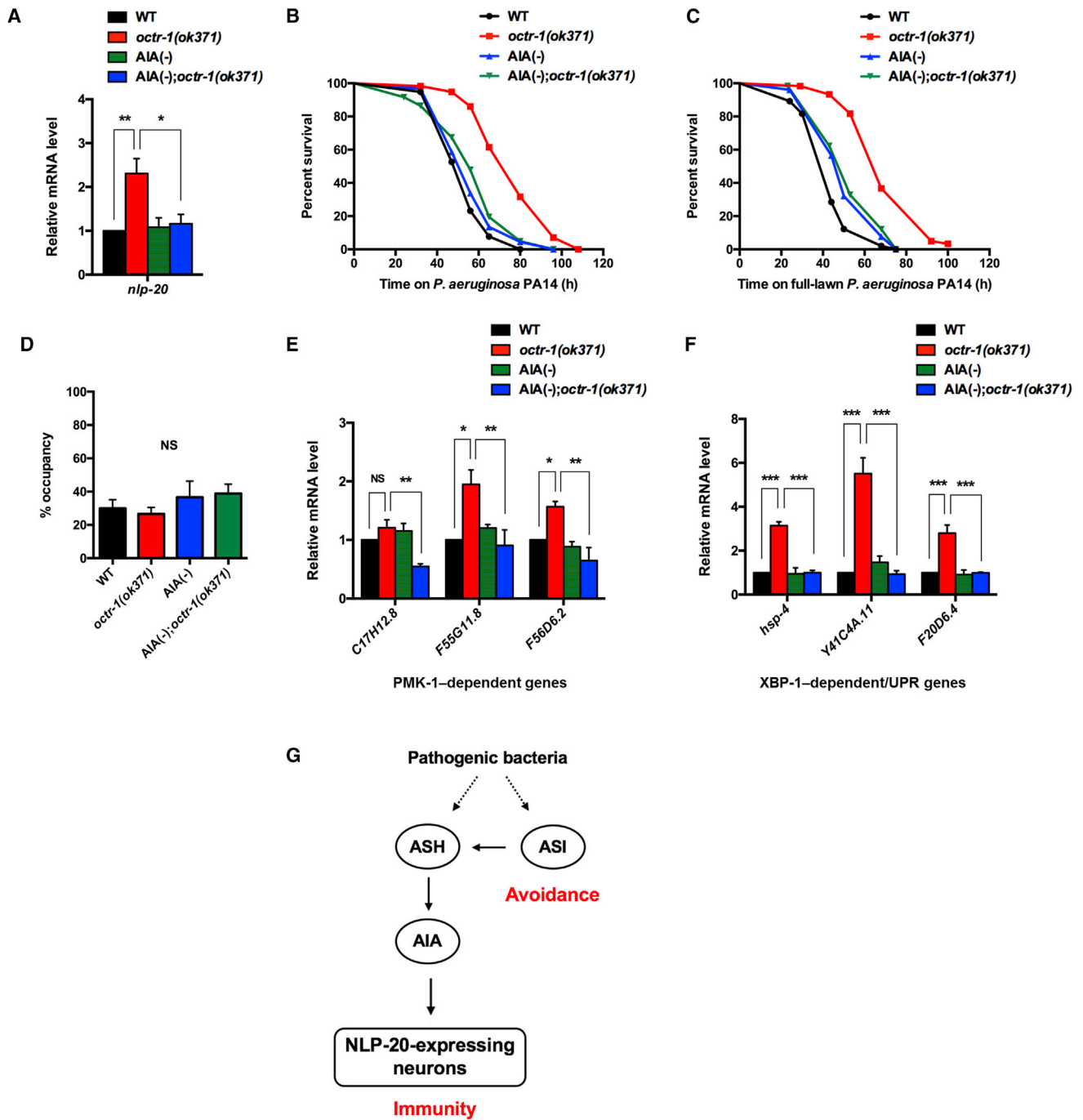


Figure 4. AIA Interneurons Are Essential for OCTR-1-Mediated Immune Regulation

(A) qRT-PCR analysis of the expression of *nlp-20* in *octr-1(ok371)*, AIA(-), and AIA(-);*octr-1(ok371)* animals compared with WT animals. (B) WT, *octr-1(ok371)*, AIA(-), and AIA(-);*octr-1(ok371)* animals were exposed to partial lawns of *P. aeruginosa* PA14 and scored for survival. AIA(-) versus AIA(-);*octr-1*, $p < 0.001$. (C) WT, *octr-1(ok371)*, AIA(-), and AIA(-);*octr-1(ok371)* animals were exposed to full lawns of *P. aeruginosa* PA14 and scored for survival. AIA(-) versus AIA(-);*octr-1*, $p < 0.001$. (D) WT, *octr-1(ok371)*, AIA(-), and AIA(-);*octr-1(ok371)* animals were cultured on partial pathogen lawns, and the percentages of animals on the pathogen lawns after incubation for 24 hr were calculated. (E) qRT-PCR analysis of PMK-1-dependent genes in *octr-1(ok371)*, AIA(-), and AIA(-);*octr-1(ok371)* animals compared with WT animals.

(legend continued on next page)

ASI neurons in mediating avoidance through the secretion of DAF-7 (Meisel et al., 2014). In the wild, *C. elegans* may evoke avoidance behavior through ASJ and ASI neurons to reduce the ingestion of pathogenic food and maintain inhibitory control of the innate immune response achieved simultaneously by the ASH neuron. The combination of the functions of the two neurons might represent a common strategy employed by living organisms that saves energy used to synthesize immune effectors by adopting avoidance behavior and prevents potential damage induced by aberrant or uncontrolled immune activation.

Here we also show that AIA neurons are required for the immune regulation of OCTR-1 in *C. elegans* by regulating expression of the neuropeptide gene *nlp-20* in downstream neurons. Interestingly, a recent study has shown that the disruption of mitochondrial function in a subset of neurons, including AIA neurons, is able to induce cell non-autonomous mitochondrial UPR in non-neural tissues via the neuropeptide FLP-12 (Shao et al., 2016). These results imply that AIA interneurons might have a broad role in integrating the aversive signals or stress conditions acquired by sensory neurons to orchestrate the systemic response in downstream cells or tissues.

Our studies have elucidated the roles of two sensory neurons, ASH and ASI, in mediating pathogen defense. We further revealed the downstream components that are essential for OCTR-1-controlled immune response. It is still unknown whether ASH and/or ASI could detect the presence of pathogens directly or through signals originated from other neurons. There is evidence showing that the octopaminergic RIC neurons are involved in the immune regulation of OCTR-1 (Liu and Sun, 2017). RIC neurons are interneurons that do not have direct contact with the environment. This suggests that additional neurons might be able to directly respond to pathogens and transmit signals to RIC neurons for the release of octopamine. Future studies might focus on elucidating the detailed molecular mechanism by which different neurons integrate signals to coordinate behavioral responses and activation of target immune genes in non-neural tissues.

EXPERIMENTAL PROCEDURES

Nematode and Bacterial Strains

C. elegans strains were cultured and maintained using standard conditions as described previously (Brenner, 1974). Bristol N2 was used as the wild-type control unless otherwise indicated. The following strains were used: VC224 *octr-1(ok371)*, RB1396 *nlp-20(ok1591)*, AY136 *octr-1(ok371);nlp-20(ok1591)*, AY137 *octr-1(ok371);nlp-20(ok1591);acEx[Pnlp-20::nlp-20::SL2::gfp]*, AY138 *octr-1(ok371);nlp-20(ok1591);acEx[Pnlp-20::gfp];acEx[Pnlp-20::ced-3(p15)*, *Pnlp-20::ced-3(p17)*, *Punc-122::gfp]*, ASI(-) PY7505 *oyls84[Pgpa-4::ced-3(p17)*, *Pgcy-27::ced-3(p15)*, *Pgcy-27::gfp*, *Punc-122::dsRed]* (Beverly et al., 2011), ASH(-) *nuEx1684[Psra-6::ced-3::gfp*, *Psra-6::mCherry*, *Pvha-6::mCherry]* (Choi et al., 2015), AIA(-) *qjEx[Pgcy-28.d::gfp];qjEx[Pgcy-28.d::mec-4(d)*, *Plin-44::gfp]* (Shinkai et al., 2011), AY139 *octr-1(ok371)*; *oyls84[Pgpa-4::ced-3(p17)*, *Pgcy-27::ced-3(p15)*, *Pgcy-27::gfp*, *Punc-122::dsRed]*, AY140 *octr-1(ok371);nuEx1684[Psra-6::ced-3::gfp*, *Psra-6::mCherry*, *Pvha-6::mCherry]*, AY141 *octr-1(ok371);qjEx[Pgcy-28.d::gfp];qjEx[Pgcy-28.d::*

mec-4(d), *Plin-44::gfp]*. The efficacy of ASH ablation was confirmed by observation of decreased levels of the L4-adult motile fraction and locomotion rate in ASH(-);*npr-1* mutants as described previously (Choi et al., 2015). The efficacy of ASI ablation was confirmed by observing the thermotaxis deficiency (Beverly et al., 2011) and the satiety quiescence of ASI(-) animals (Gallagher et al., 2013). The efficacy of AIA ablation has been confirmed by the resulting defective response to the integrated stimuli of Cu²⁺ and diacetyl (Shinkai et al., 2011). The following bacterial strains were used: *Escherichia coli* strain OP50 (Brenner, 1974) and *Pseudomonas aeruginosa* strain PA14 (Tan et al., 1999). Bacterial cultures were grown overnight in 4 mL of Luria-Bertani (LB) broth at 37°C.

C. elegans Killing and Longevity Assays

The bacterial lawns used for the *C. elegans* killing assays were prepared by placing 20 μ L of an overnight culture of the bacterial strains on modified nematode growth media (NGM) agar medium (0.35% instead of 0.25% peptone) in 3.5-cm-diameter plates. The plates were incubated overnight at 37°C and cooled to room temperature for 1 hr before being seeded with animals. Full-lawn plates were prepared by spreading 50 μ L of overnight culture over the complete surface of modified NGM agar medium in 3.5-cm-diameter plates. For longevity assays, the overnight cultures of *E. coli* OP50 were concentrated at a 1:10 ratio and heat-killed at 100°C for at least 1 hr. Animals were synchronized by placing gravid adults on NGM plates containing *E. coli* OP50 for 2 hr at 25°C. The gravid adults were removed, leaving the eggs to hatch and develop at 20°C. Synchronized young adult *C. elegans* hermaphrodites were transferred to modified NGM plates containing bacterial lawns and incubated at 25°C. Animals were scored at the indicated times for survival and transferred to fresh pathogen lawns each day until no progeny was produced. Animals were considered dead when they failed to respond to touch and no pharyngeal pumping was observed. Each experiment was performed in triplicate (n = 60 animals).

Pathogen Avoidance Assay

The bacterial lawns were prepared as described above. Thirty synchronized young adult *C. elegans* hermaphrodites were transferred to bacterial lawns, and the plates were incubated at 25°C for 24 hr before counting. The avoidance behavior of each strain was quantified based on the fraction of animals on the bacterial lawn.

RNA Isolation and qRT-PCR

Synchronized L1 larval animals were placed on NGM plates seeded with *E. coli* OP50 and grown at 20°C until the animals reached the L4 larval stage (for PMK-1-dependent genes) or 1-day-old adult stage (for XBP-1-dependent genes). Animals were collected and washed with M9 buffer before being transferred to modified NGM plates containing *P. aeruginosa* PA14 or *E. coli* OP50 for 4 hr at 25°C. Animals were washed off the plates with M9 and frozen in TRIzol by ethanol/dry ice. Total RNA was extracted, and residual genomic DNA was removed. The relative fold changes of the transcripts were calculated using the comparative C_T (2^{- $\Delta\Delta$ CT}) method and normalized to pan-actin.

Cell Identification by Fluorescence Microscopy

The identification of cells expressing the *gfp* reporter gene under the control of the *nlp-20* promoter was confirmed by cell position and axon morphology. A dye-filling assay was performed using Vybrant DiD cell-labeling solution to visualize amphid and phasmid neurons as a landmark for the relative cell position, following the method described in WormBook (Shaham, 2006). Briefly, a stock solution of DiD was diluted 1:100 in M9 buffer. Young adult animals were transferred into the dye solution and incubated at room temperature for 2 hr. Animals were then pelleted and plated onto fresh plates seeded with *E. coli* OP50 for 15 min for destaining. Animals were then mounted on a 2% (w/v) agar pad and observed using a Zeiss Axioskop2 Mot Plus microscope

(F) qRT-PCR analysis of XBP-1-dependent genes in *octr-1(ok371)*, AIA(-), and AIA(-);*octr-1(ok371)* animals compared with WT animals.

(G) Schematic showing the neuronal coordination of immunity and avoidance. Arrows indicate neuronal connections, including chemical synapses and gap junctions, whereas dashed arrows indicate sensory inputs.

See also Figure S4.

equipped with AxioVision v3.1 imaging software and a Leica TCS SL confocal microscope equipped with Leica confocal software version 2.61 Build 1537.

Statistical Analysis

Survival curves were plotted using GraphPad Prism 6 (GraphPad, La Jolla, CA). Survival curves were considered different from the control when $p < 0.05$. The Kaplan-Meier method was used to calculate the survival fractions, and statistical significance between survival curves was determined using the log-rank test. One-way ANOVA was used to determine the statistical significance among groups of data, with Bonferroni correction for multiple comparisons, and $p < 0.05$ was considered significant. All experiments were conducted in triplicate. All bars represent means \pm SEM; * $p < 0.05$, ** $p < 0.01$, *** $p < 0.001$; NS, not significant.

SUPPLEMENTAL INFORMATION

Supplemental Information includes four figures and can be found with this article online at <https://doi.org/10.1016/j.celrep.2017.10.050>.

AUTHOR CONTRIBUTIONS

X.C., R.K.-S., and A.A. conceived and designed the experiments. X.C., R.K.-S., and A.D. performed the experiments. X.C. and A.A. analyzed the data and wrote the paper.

ACKNOWLEDGMENTS

This work was supported by NIH grants GM0709077 and AI117911 (to A.A.). Some strains used in this study were provided by the Caenorhabditis Genetics Center (CGC), which is funded by the NIH Office of Research Infrastructure Programs (P40 OD010440). We thank the *C. elegans* Gene Knockout Project at OMRF for the strains used in this work, Kaveh Ashrafi (UCSF, San Francisco, CA) for providing the *Pmgl-1::mCherry* plasmid, Joshua Kaplan (Harvard Medical School, Boston, MA) for providing the strain KP7442, and Takeshi Ishihara (Kyushu University, Fukuoka, Japan) for providing the AIA(-) strain.

Received: July 19, 2017

Revised: September 19, 2017

Accepted: October 13, 2017

Published: November 7, 2017

REFERENCES

Akira, S., Uematsu, S., and Takeuchi, O. (2006). Pathogen recognition and innate immunity. *Cell* 124, 783–801.

Beverly, M., Anbil, S., and Sengupta, P. (2011). Degeneracy and neuromodulation among thermosensory neurons contribute to robust thermosensory behaviors in *Caenorhabditis elegans*. *J. Neurosci.* 31, 11718–11727.

Brenner, S. (1974). The genetics of *Caenorhabditis elegans*. *Genetics* 77, 71–94.

Cao, X., and Aballay, A. (2016). Neural Inhibition of Dopaminergic Signaling Enhances Immunity in a Cell-Non-autonomous Manner. *Curr. Biol.* 26, 2329–2334.

Choi, S., Taylor, K.P., Chatzigeorgiou, M., Hu, Z., Schafer, W.R., and Kaplan, J.M. (2015). Sensory Neurons Arouse *C. elegans* Locomotion via Both Glutamate and Neuropeptide Release. *PLoS Genet.* 11, e1005359.

Curtis, V.A. (2014). Infection-avoidance behaviour in humans and other animals. *Trends Immunol.* 35, 457–464.

Flajnik, M.F., and Kasahara, M. (2010). Origin and evolution of the adaptive immune system: genetic events and selective pressures. *Nat. Rev. Genet.* 11, 47–59.

Gallagher, T., Kim, J., Oldenbroek, M., Kerr, R., and You, Y.-J. (2013). ASI regulates satiety quiescence in *C. elegans*. *J. Neurosci.* 33, 9716–9724.

Greer, E.R., Pérez, C.L., Van Gilst, M.R., Lee, B.H., and Ashrafi, K. (2008). Neural and molecular dissection of a *C. elegans* sensory circuit that regulates fat and feeding. *Cell Metab.* 8, 118–131.

Grootjans, J., Kaser, A., Kaufman, R.J., and Blumberg, R.S. (2016). The unfolded protein response in immunity and inflammation. *Nat. Rev. Immunol.* 16, 469–484.

Guo, M., Wu, T.-H., Song, Y.-X., Ge, M.-H., Su, C.-M., Niu, W.-P., Li, L.-L., Xu, Z.-J., Ge, C.-L., Al-Mhanawi, M.T., et al. (2015). Reciprocal inhibition between sensory ASH and ASI neurons modulates nociception and avoidance in *Caenorhabditis elegans*. *Nat. Commun.* 6, 5655.

Inglis, P.N., Ou, G., Leroux, M.R., and Scholey, J.M. (2007). The sensory cilia of *Caenorhabditis elegans*. *WormBook*, 1–22.

Iwasaki, A., and Medzhitov, R. (2010). Regulation of adaptive immunity by the innate immune system. *Science* 327, 291–295.

Kavaliers, M., and Choleris, E. (2011). Sociality, pathogen avoidance, and the neuropeptides oxytocin and arginine vasopressin. *Psychol. Sci.* 22, 1367–1374.

Lefkowitz, R.J. (2013). A brief history of G-protein coupled receptors (Nobel Lecture). *Angew. Chem. Int. Ed. Engl.* 52, 6366–6378.

Liu, Y., and Sun, J. (2017). G Protein-Coupled Receptors Mediate Neural Regulation of Innate Immune Responses in *Caenorhabditis elegans*. *Receptors Clin. Investig.* 4, e1543.

Martin, N., Singh, J., and Aballay, A. (2017). Natural genetic variation in the *Caenorhabditis elegans* response to *Pseudomonas aeruginosa*. *G3* 7, 1137–1147.

Meisel, J.D., and Kim, D.H. (2014). Behavioral avoidance of pathogenic bacteria by *Caenorhabditis elegans*. *Trends Immunol.* 35, 465–470.

Meisel, J.D., Panda, O., Mahanti, P., Schroeder, F.C., and Kim, D.H. (2014). Chemosensation of bacterial secondary metabolites modulates neuroendocrine signaling and behavior of *C. elegans*. *Cell* 159, 267–280.

Pancer, Z., and Cooper, M.D. (2006). The evolution of adaptive immunity. *Annu. Rev. Immunol.* 24, 497–518.

Pradel, E., Zhang, Y., Pujol, N., Matsuyama, T., Bargmann, C.I., and Ewbank, J.J. (2007). Detection and avoidance of a natural product from the pathogenic bacterium *Serratia marcescens* by *Caenorhabditis elegans*. *Proc. Natl. Acad. Sci. USA* 104, 2295–2300.

Reddy, K.C., Andersen, E.C., Kruglyak, L., and Kim, D.H. (2009). A polymorphism in *npr-1* is a behavioral determinant of pathogen susceptibility in *C. elegans*. *Science* 323, 382–384.

Shaham, S. (2006). *Methods in cell biology*. WormBook.

Shao, L.-W., Niu, R., and Liu, Y. (2016). Neuropeptide signals cell non-autonomous mitochondrial unfolded protein response. *Cell Res.* 26, 1182–1196.

Shinkai, Y., Yamamoto, Y., Fujiwara, M., Tabata, T., Murayama, T., Hirotsu, T., Ikeda, D.D., Tsunozaki, M., Iino, Y., Bargmann, C.I., et al. (2011). Behavioral choice between conflicting alternatives is regulated by a receptor guanylyl cyclase, GCY-28, and a receptor tyrosine kinase, SCD-2, in AIA interneurons of *Caenorhabditis elegans*. *J. Neurosci.* 31, 3007–3015.

Sironi, M., Cagliani, R., Forni, D., and Clerici, M. (2015). Evolutionary insights into host-pathogen interactions from mammalian sequence data. *Nat. Rev. Genet.* 16, 224–236.

Styer, K.L., Singh, V., Macosko, E., Steele, S.E., Bargmann, C.I., and Aballay, A. (2008). Innate immunity in *Caenorhabditis elegans* is regulated by neurons expressing NPR-1/GPCR. *Science* 322, 460–464.

Sun, J., Singh, V., Kajino-Sakamoto, R., and Aballay, A. (2011). Neuronal GPCR controls innate immunity by regulating noncanonical unfolded protein response genes. *Science* 332, 729–732.

Sun, J., Liu, Y., and Aballay, A. (2012). Organismal regulation of XBP-1-mediated unfolded protein response during development and immune activation. *EMBO Rep.* 13, 855–860.

Tan, M.W., Mahajan-Miklos, S., and Ausubel, F.M. (1999). Killing of *Caenorhabditis elegans* by *Pseudomonas aeruginosa* used to model mammalian bacterial pathogenesis. *Proc. Natl. Acad. Sci. USA* 96, 715–720.

Tomioka, M., Adachi, T., Suzuki, H., Kunitomo, H., Schafer, W.R., and Iino, Y. (2006). The insulin/PI 3-kinase pathway regulates salt chemotaxis learning in *Caenorhabditis elegans*. *Neuron* 51, 613–625.

Troemel, E.R., Chu, S.W., Reinke, V., Lee, S.S., Ausubel, F.M., and Kim, D.H. (2006). p38 MAPK regulates expression of immune response genes and contributes to longevity in *C. elegans*. *PLoS Genet.* 2, e183.

Urano, F., Calfon, M., Yoneda, T., Yun, C., Kiraly, M., Clark, S.G., and Ron, D. (2002). A survival pathway for *Caenorhabditis elegans* with a blocked unfolded protein response. *J. Cell Biol.* 158, 639–646.

White, J.G., Southgate, E., Thomson, J.N., and Brenner, S. (1986). The structure of the nervous system of the nematode *Caenorhabditis elegans*. *Philos. Trans. R. Soc. Lond. B Biol. Sci.* 314, 1–340.

Xiao, H., Hapiak, V.M., Smith, K.A., Lin, L., Hobson, R.J., Plenefisch, J., and Komuniecki, R. (2006). SER-1, a *Caenorhabditis elegans* 5-HT₂-like receptor, and a multi-PDZ domain containing protein (MPZ-1) interact in vulval muscle to facilitate serotonin-stimulated egg-laying. *Dev. Biol.* 298, 379–391.